Evaluation of different metal cutting models during machining of Inconel-718

Author

Muhammad Ghazi Hamza

Reg Number

320330

Supervisor

Dr. Syed Hussain Imran Jaffery

DEPARTMENT

SCHOOL OF MECHANICAL & MANUFACTURING ENGINEERING

NATIONAL UNIVERSITY OF SCIENCES AND TECHNOLOGY

ISLAMABAD

JULY 2022

Evaluation of different metal cutting models during machining of Inconel-718

Author

Muhammad Ghazi Hamza

Reg Number

320330

A thesis submitted in partial fulfillment of the requirements for the degree of

MS Mechanical Engineering

Thesis Supervisor:

Dr. Syed Hussain Imran Jaffery

Thesis Supervisor's Signature: ____

DEPARTMENT

SCHOOL OF MECHANICAL & MANUFACTURING ENGINEERING

NATIONAL UNIVERSITY OF SCIENCES AND TECHNOLOGY,

ISLAMABAD

JULY 2022

Declaration

I certify that this research work titled "*Evaluation of different metal cutting models during machining of Inconel-718"* is my own work. The work has not been presented elsewhere for assessment. The material that has been used from other sources it has been properly acknowledged / referred.

Signature of Student

Muhammad Ghazi Hamza

2019-NUST-MS-Mech-320330

Plagiarism Certificate (Turnitin Report)

This thesis has been checked for Plagiarism. Turnitin report endorsed by Supervisor is attached.

Signature of Student

Muhammad Ghazi Hamza

Registration Number

320330

Signature of Supervisor

Copyright Statement

Acknowledgements

First of all, I want to express my utmost gratitude towards Allah, the most merciful and the most beneficent, for blessing me with the opportunity and knowledge that enabled me to start this research work and enabled me to finish this task in the given time. Without his blessing and guidance, I would not have been able to accomplish this task. His mercy and blessings helped on each and every step of this process and made be able to complete my thesis.

I want to express my gratitude towards my parents and all family members for supporting me on every step of life and being a source of motivation and support throughout this process. They have been the source of my emotional support on each difficult step as well whenever I faced a setback during this journey.

I am thankful to my supervisor Dr. Syed Hussain Imran Jaffery for his guidance and support throughout the journey of this research work. He was very helpful by providing guidance on each step and for pointing me towards the right direction in search for the solution every time I got stuck or faced a problem which I deemed to be very complex and problematic. He has been a source of motivation for me and also an excellent teacher in the field of Materials.

I would also like to thank the administration and faculty of SMME for providing an atmosphere of learning and the appropriate resources that proved to be helpful in this journey.

Dedicated to my parents and all members of my family who have been a source of support and motivation and helped me through every phase of life.

Abstract

Inconel-718 is a nickel-based aerospace alloy that has large domain of applications in the aerospace industry and also in ground-based turbines. Machining of Inconel-718 is a very difficult process as it is able to retain its strength even at high temperatures resulting in a lot of tool wear and making it difficult to machine, thus making it a topic of interest among researchers. In order to study the orthogonal machining process of this material, development of a FEM model, in Abaqus software, which can simulate the process with good accuracy is extremely important. To simulate the plastic deformation and damage of Inconel-718, during the machining process, different material modelling techniques are available in the literature. Among these material models, Johnson Cook Plasticity model is widely accepted as being more accurate. When modelling the machining process using FEM, the Johnson Cook Plasticity model is utilized to forecast the plastic deformation and behaviour of a material. However, there are different values of parameters, involved in the JC model equation, available in the literature which have been derived experimentally. Using these different values of parameters in the simulation process of machining brings a variation in the output values. Thus, the need to evaluate these different models arises. This research will focus on identifying which model proves to be more accurate in predicting the cutting forces during machining of Inconel-718. Results obtained from each model will be compared to the experimental results and a conclusion will be derived about which model is preferrable to be used in simulation this process in future.

Key Words: *Orthogonal machining process, Finite Element Modelling, Aerospace Alloys, Johnson Cook Material Model, Inconel 718*

Table of Contents

List of Figures

List of Tables

Chapter 1: Introduction

Metal cutting and machining process hold a great significance in the field of engineering materials owing to their crucial role in the industry. Every field of engineering is related to the material cutting and machining process somehow. Research have been working on several methods and techniques to optimize the machining process and trying to simulate the behavior of materials to learn about their elastic and plastic deformations and how they affect the tool. Many factors including cutting force, feed force, temperature and chip morphology effect the machining process. However, cutting force is the prominent factor that contributes the most to the tool wear. Experimentally cutting force can be calculated using dynamometers and theoretically it can be calculated using mathematical modeling. Different finite element softwares are also available to simulate the machining process and predict accurate cutting forces thus reducing the amount of funds required to perform calculations using experimental setup. Prediction of cutting forces is very vital for designing of cutting tool and overall optimization of the process of machining .

Machining of Aerospace alloys specially Inconel-718 is a very difficult and expensive process as they have high strengths and they do not deform easily, and they have the ability to retain their properties on very high temperatures. This phenomenon makes them difficult to machine and cause a lot of tool wear. To study and improves the efficient of machining, the cost of experimentation can be reduced by simulation the machining process using FEM. This allows the researchers to study the behavior of materials during machining at low cost.

Many material modeling techniques are available in the literature which can be used to simulate the behavior of metal during FEA analysis of orthogonal machining process. However, the JC plasticity model is the most widely accepted and utilized model in this manner. The purpose of this research is to evaluate different values of JC model parameters available in the literature and form a conclusion about which model brings the simulation results as close to the experimental results as possible for the orthogonal machining process of an aerospace alloy called Inconel 718.

First let’s discuss what are aerospace alloys and their significance in the field of engineering and aerospace industry.

1.1 Aerospace alloys:

Aviation and space industry are very high investment and advanced industries. Safety and durability hold high significance in these domains as compared to other fields. As the aircraft and rocket components must go through rigorous conditions involving high speed, very high and very low temperatures. The materials used in these components need to have excellent mechanical and thermal properties to withstand such working conditions without compromising the integrity of the structure and also being economically viable for the business. The researchers continuously work on developing materials and alloys, by combining different materials have desirable properties which can provide such kind of performance and also make the overall operation lighter and cheaper. Superalloys are also used in this regard.

There are many materials available in the market now. There are more than 120,000 materials from which engineers can choose while designing an aircraft [1]. The aerospace alloys are designed to exhibit extraordinary performance in heat resistance or strength and durability even when they are highly expensive to produce and are very difficult to machine.

Aerospace alloys comprise of different materials including Al- and Mg-, Ni-, Co- and Ti-based alloys [2]. Certain elements are added to the case element to produce these alloys with the desired characteristics. Due to their excellent performance in aerospace industries, other branches of engineering have also started to explore and use these alloys in their operations.

1.2 Commercial Importance

It is a basic requirement for the Materials being used in the gas turbine engines to operate under high operating temperatures and stresses for a prolonged period [2]. Similarly, aircrafts must operate in very harsh conditions like extreme temperatures (both high and very low), high air resistance and vibrations. Any impact from even a small object at such high speeds can cause severe damage to the integrity of the structure. So, the need for development of materials which can cater to these high demands is crucial for advancement in aerospace industry and make this industry sustainable. Certain alloys have been developed which can meet these demands while not having the limitations of ordinary metals. They combine the beneficial characteristics of different materials which reducing their negative traits. Thus, aerospace alloys have a high commercial demand. The aerospace industry is evolving rapidly and continuously trying to make their operations more economic by weight reduction, inducing components that have high fatigue resistance and corrosion resistance and are more durable than ordinary metals. Such demands can only be fulfilled by aerospace alloys which are designed specifically for these purposes. Aerospace industry has a huge contribution in carbon emissions and different factors that contribute to global warming, as a result companies are in effort to reduce the overall weight of their aircrafts to reduce fuel consumption and thus reducing their overall emissions. Aerospace alloys are critical for this process. They are important and useful because of their long lifespan and reliability.

1.3 Usage

Due to their exceptional performance and excellent characteristics, different aerospace alloys are being used widely in various branches of aerospace industry. Choosing the best material which fulfills the requirements while keep the whole business sustainable economically is the critical decision for aerospace engineers and designers.

Al-based alloys are used in the fuselage of aircrafts, wing skins and other non-structural components of aircrafts. Specially designed alloys are used in making parts used in jet engines and airframes [2]. Al-based alloys are used in the upper wing skins of aircrafts to withstand high bending loads [3].Due to their good corrosion resistance, excellent structural properties and their ability to retain their properties at high temperatures, Titanium alloys are widely used in aircraft components. Specially in fighter aircrafts. Titanium-based alloys account for 25-30% of the weight of engines of modern jets [3]. Nickel-based alloys are readily used in the components of jet engines for their proven ability to withstand high temperatures, corrosion, and wear and also for their good magnetic properties. They are structurally some of the toughest materials available.

1.4 Properties of aerospace alloys and Inconel 718

There are certain requirements which make aerospace industry different from other engineering disciplines. As the operating conditions are very harsh and extreme, the aerospace alloys provide such properties that are suitable for such requirements. Generally aerospace alloys offer good strength-to-weight ratio, good resistance against corrosion, high structural strengths, ability to perform under high temperatures without losing their advantage, durability.

Table 1: Properties of certain aerospace alloys at room temperature [4] [1] [5]

Property	**Material**						
	Titanium	**Ti-6Al-4V**	**Ti-6Al-6V-2Sn**	**Ti-8V-6Cr-4months-4Zr-3Al**	**Ti-10V-2Fe-3Al**	**Inconel 718**	**Al 7075 – T6 Alloy**
Density (g/cm^3)	4.5	4.43	4.54	4.81	4.65	8.22	2.81
Hardness (HRc)	10-12	30-36	38	37-43	32	38-44	~7
Ultimate Tensile Strength (MPa)	220	950	1050	1250	970	1350	572
Yield Strength (MPa)	140	880	980	1150	900	1170	503
Modulus of Elasticity (GPa)	116	113.8	110	102	110	200	71.7
Ductility (%)	54	14	14	15	9	16	11
Fracture toughness ($MPa\ m^{1/2}$)	70	75	60	65	-	96.4	20-29
Thermal conductivity (W/mK)	17	6.7	6.6	8.4	7.8	11.4	130
Maximum operating temperature (^oC)	~150	315	315	315	315	650	-

1.5 Inconel 718 and its importance and usage

Inconel is a trademark of Special Metal Corporation for the family of austenitic nickel-chromium based alloys. They are well known for their corrosion and oxidation resistance properties while operating at high temperatures and high mechanical loads. The material under discussion in this research work in Inconel 718 which is a part of the Inconel family of alloys. It is a corrosion resistant, high strength nickel chromium alloy which can be used between -423^{o} F to 1300^{o} F. Inconel-718 is a Nickel based superalloy. Many superalloys have substantial amount of three or more metals.

Table 2: Chemical composition of Inconel-718 is as following: [6]

Element	Percentage Chemical Composition
Nickel	50 - 55
Chromium	17 - 21
Iron	Balance
Niobium (plus Tantalum)	4.75 – 5.50
Molybdenum	2.80 – 3.30
Titanium	0.65 – 1.15
Aluminum	0.20 – 0.80
Cobalt	1.00 max.
Carbon	0.08 max.
Manganese	0.35 max.
Silicon	0.35 max.
Phosphorus	0.015 max.
Sulphur	0.015 max.
Boron	0.006 max.
Copper	0.30 max.

Nickel based superalloys have better strength at high temperatures as compared to alloy steels. The excellent properties of Inconel 718 have made it useful in diverse applications such as making components of liquid fuel rockets, rings, castings, and parts of aircrafts made from sheet metal, engines of gas turbines and cryogenic tankage [6]. Such excellent properties and usage of this material makes it a topic of research for scientists and engineers.

As currently there is no alternate available which can replace Inconel 718. Researcher are working to improve its machinability and explore further usage of this material in the industry.

Figure 1: A sample of Inconel-718

1.6 Machinability

Machining of Inconel 718 is a difficult process. Aerospace industry used Inconel-718 extensively because of its known ability for retaining its mechanical properties even at high temperatures up to 700^{o}C which also makes it difficult to machine. These qualities contribute towards higher values of cutting forces and high temperatures during the cutting process which lead to high tool wear. Cutting force acts as a major contributor in heat generation [7]. This material is used extensively in the aerospace industry and has a promising future in other fields of engineering as well however, the difficulties in its machining process pose a challenge for its use in making more complex shapes and low budget applications, thus researchers are continuously working on making the machining process of this material more easy, efficient, and economical so its application can be broadened. Making an accurate FEM model which can simulate the machinability of Inconel 718 contributes to this effort.

1.7 Metal cutting processes:

Metal cutting involves removal of excess or unwanted material from a workpiece by exerting an external force using a tool which initiates fracture in the workpiece as a result the unwanted material gets removed in the form of chips. The movement of tool further along the workpiece results in the material getting deformed by shear stress. Metal cutting process are an integral part of engineering sciences and industry and always under the consideration of researchers to optimize this process to make it more efficient.

There are mainly two types of metal cutting processes:

1) Oblique cutting process
2) Orthogonal cutting process

1.7.1 Oblique Cutting process:

In this process, the cutting tool makes an oblique angle with the direction of its motion. In this process the cutting tool edge has a long cutting life as compared to the other. There is low shear force per unit in this process resulting in less heat generation. Good surface finish is resulted in case of oblique cutting process. The force acting on the top of tool has three components (cutting force 'F_C', feed force 'F_d', radial force 'F_r') are considered in this type of cutting process which makes it impossible to be represented in 2D coordinate system during simulation.

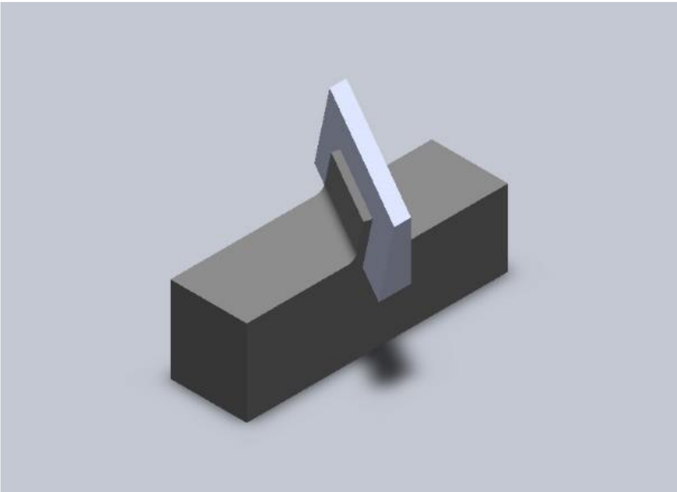

Figure 2: Oblique Cutting process

1.7.2 Orthogonal cutting process:

In this process, the cutting tool edge is at a right angle to direction of its motion. In this process, tool has a low cutting life. Flow of chips is perpendicular to the cutting edge. Due to high shear force per unit area, increase in heat generation per unit area is observed. Orthogonal cutting results in poor surface finish. In orthogonal cutting process, two components of force (cutting force 'F_C', feed force 'F_r') acting on the tool tip are under consideration which makes it possible to represent this process in two-dimensional modeling thus the FEA model developed in this research work will be developed in 2D.

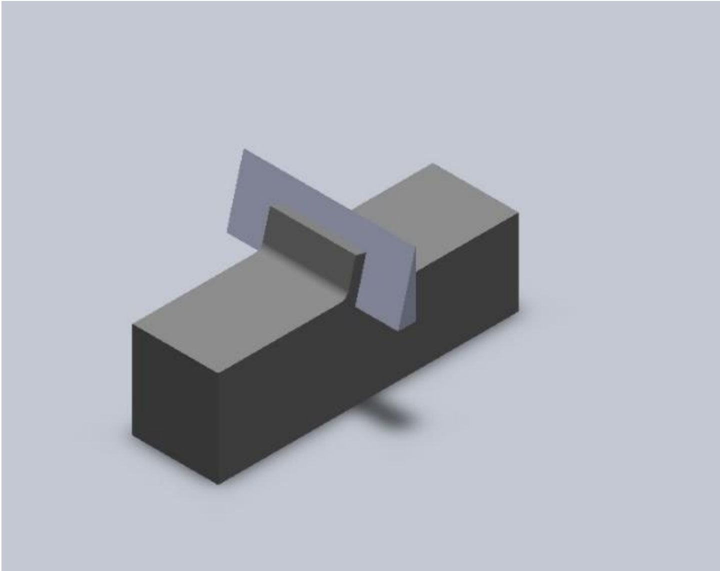

Figure 3: Orthogonal cutting process

1.8 FEM Modelling

FEM is often used to obtain knowledge about the performance and associated mechanisms of the cutting processes [8]. The correct prediction of forces acting on tool proves to be of crucial importance in understanding the machining processes and tool design. In finite element method a continuum is divided into a finite number of discrete and interdependent problems. There are many commercial softwares available in the market which are used to simulate the process of orthogonal machining. However, Abaqus explicit is mostly used by researchers and in this research work Abaqus Explicit will be used to develop a 2D FEA model of orthogonal cutting process. This model will be able to simulate machining process of Inconel 718 and give detailed results of the output parameters.

There are three common methods while meshing of the model and its motion i.e., Lagrangian, Eulerian and Arbitrary Lagrangian-Eulerian (ALE). In the Lagrangian method, mesh grid moves with the material points. It lacks the ability to simulate models with large deformations. In Eulerian method, material moves through the mesh grid while the mesh grid is fixed in position. It can simulate large deformations, but the material flow must be defined before simulation. ALE method combines the pros of both above mentioned methods while avoiding the disadvantages of both. So, it proves to be more beneficial while simulating the machining processes involving large deformation. It maintains a topologically similar mesh throughout the analysis [9].

1.9 Material Models

Defining the material properties and modelling its elastic and plastic deformation behaviour is an important step in simulation of machining process. There are certain material modelling techniques available in the literature which can be used while performing FEA analysis of material during machining processes. Among these models the following are widely used in metal cutting process modeling:

1. Johnson Cook model
2. Oxley model
3. Zerilli-Armstrong model

1.9.1 Johnson-Cook Plasticity Model

There are different material modelling methods available in the literature which can be used to predict the stresses and plastic deformation during the cutting processes of different materials. However, Gordon R. Johnson and William H. Cook develop a fracture model to determine the fracture characteristics of different materials [10]. Johnson-cook model is widely accepted among researchers due to its ability for predicting the plastic deformation behavior of metals in processes that involve high strain rates, large strains and high temperature deformations [7].

The equation for Johnson Cook model plasticity model is as follows:

$$\sigma = (A + B\varepsilon^{n})(1 + C\ln\frac{\dot{\varepsilon}}{\dot{\varepsilon_o}})(1 - \left(\frac{T - T_{room}}{T_{melt} - T_{room}}\right)^{m})$$

where A is yield strength, B is strain hardening parameter, C is strain rate constant, n is strain hardening exponent, m is the thermal softening exponent while T_{room} represents room temperature and T_{melt} represents melting temperature and T stands for reference temperature and ε represents equivalent plastic strain and $\dot{\varepsilon_o}$ is reference equivalent plastic strain rate. It can be noted that this equation consists of three portions. First portion defines strain hardening effects, second portion represents strain rate dependence, and third portion will define the temperature softening effects.

Johnson Cook failure defines a damage parameter 'W' for this purpose. Failure occurs when the value of damage parameter W exceeds the value of 1.The failure parameter can be defined as:

$$W = \sum \left(\frac{\Delta\in^{pl}}{\in_f^{pl}}\right)$$

Where $\Delta\in^{pl}$ is the increase in plastic strain and $\in_f^{pl}$is failure strain.

To model the damage initiation process, JC damage model is used. The equivalent strain at failure for Johnson Cook damage model is as follows:

$$\varepsilon_f = \left[\left(D_1 + D_2 \exp\left(D_3 \frac{P}{\sigma}\right)\left(1 + D_4 ln \frac{\varepsilon_{pl}}{\varepsilon_0}\right)\right)\right][1 + D_5(\frac{T - T_r}{T_m - T_r})]$$

In this equation D_1 - D_5 are damage parameters which can be determined experimentally at transition temperature of material usually using tensile Split Hopkinson bar test or bar test [11].

It is widely accepted by most research articles that Johnson cook plasticity model is very suitable for performing analysis that involve high strain rate deformation.

1.9.2 Oxley model

Oxley Material model uses power law to represent material flow stress [12].

$$\sigma = \sigma_1 \varepsilon^n$$

Where σ and ε are flow stress and strain and σ_1 is the flow stress at ε = 1 and n is the strain hardening exponent.

Here n, σ_1 are dependent upon the velocity modified temperature (T_{mod}), which can be calculated as following:

$$T_{mod} = T(1 - v \; log \frac{\dot{\varepsilon}}{\dot{\varepsilon_o}})$$

1.9.3 Zerilli-Armstrong model

To determine the flow stress in a material, Zerilli and Armstrong presented a constitutive relation based on dislocation mechanics, which is expressed as,

$$\sigma = C_o + C_1(\varepsilon)^n \exp(-C_2 T + C_3 T ln\, \dot{\varepsilon})$$

Here σ is Von Mises Flow stress, ε is equivalent plastic strain, $\dot{\varepsilon}$ is equivalent strain rate, T is the absolute temperature of workpiece and C_0 , C_1, C_2, C_3 and n are material parameters.

1.10 Research Motivation

The motivation for this research is to find out which set of available parameters of JC model provide us with more accurate results during simulation of orthogonal machining process of Inconel 718 and that model can be used as a substitute for the experimental process and could be used to optimize the machining techniques of Inconel-718 and reduce the experimental costs during this process in the lab. Accurate FEA model of this cutting process will result in saving funds and experimental costs of the institute and prove beneficial for the optimization of tool design process.

Chapter 2: Literature Review

Machining processes and its simulation has been a topic of great interest for researchers. [13] presented methodology to predict tool wear in orthogonal machining process using FEA and proved the ability of FEA to simulation the machining process and predict wear. In orthogonal machining, the largest component of force acting on tool is the cutting force. In machining of Inconel-718, the magnitude of cutting forces is usually two or three times higher as compared to the other components of force [14]. Different material modelling techniques have been discussed in various research articles. Gordon R. Johnson and William H. Cook developed a model to determine the plastic deformation behaviour and fracture characteristics of different materials [7].

Different parameters and modifications of J-C models are available in the literature to model the material during FEM simulation process and each model affects the accuracy of the results obtained. However, there are different values of parameters available in the literature for that JC model for Inconel 718 material. So, in this research 8 different set of available values have been compiled from literature and simulation has been carried out to find the best set or input parameters of JC model to bring the most accurate results during simulation.

The values for parameters of JC material model used for comparison in this research have been gathered from models used in following research works [7], [8], [11], [15], [16], [17], [18]. Damage criterion is also very important in simulating the chip formation and element deletion in Abaqus. [19] concluded that damage criterion is necessary to trigger element deletion after severe localized deformation. It is better to predict chip morphology as compared to shear failure criteria. [13] concluded that Arbitrary Lagrangian-Eulerian (ALE) method has the advantages of both Lagrangian technique and Eulerian technique to control the distortion of the elements in problems involving large deformation i.e., chip formation, thus it is used in this research work while meshing the workpiece. Lagrangian (LAG) and ALE techniques were used to determine cutting forces in orthogonal machining and ALE was able to predict the results with more accuracy and less percentage error [20]. Excessive mesh distortion in metal cutting simulation can be controlled by adaptive meshing in FEA and also increase accuracy of ALE results [21].

Chapter 3: Development of Finite Element Model in Abaqus

In this portion, steps and techniques for development of finite element model are discussed. As in orthogonal cutting process only two components of force acting on tool are considered. Thus, this process can be simulated in 2D which reduces the computation time and cost as compared to analysis in 3D. A 2D model has been developed in the Abaqus Explicit software for simulating the process of orthogonal machining. This process included modelling the workpiece and tool geometry and defining their material properties to simulate their physical behavior and applying the loading conditions as well as other parameters required to make the model as close to the real machining process as possible.

3.1 Workpiece and tool geometry development in 2D

In the first step the geometry of workpiece and tool was developed as illustrated in the figure 4. Both the work piece and tool were modeled as two-dimensional deformable entities. In reality, orthogonal machining is a 3-dimensional process, however, we are considering a very small portion of the material which can be assumed as a straight piece and converted the process to 2D. As discussed earlier , in orthogonal machining process two main components of forces acting on the tool are considered thus this process can be simulated using a 2D model.

A small portion of the workpiece having dimension of 4mm and 2mm. The surface of workpiece was divided into 2 portions. The upper portion was meshed with a finer mesh size of 0.002 mm for the better prediction of output parameters. While the lower portion was meshed with less fine mesh of 0.02mm to reduce the computational time. The simulation duration is decreased by using a small, dense mesh area beneath the tool's penetration line in the workpiece. 4-node plane strain thermally coupled quadrilateral, bilinear displacement and temperature, reduced integration, hourglass control (CPE4RT) elements were utilized in the meshing of the workpiece. The mesh was verified and had an average aspect ratio of 1.89.

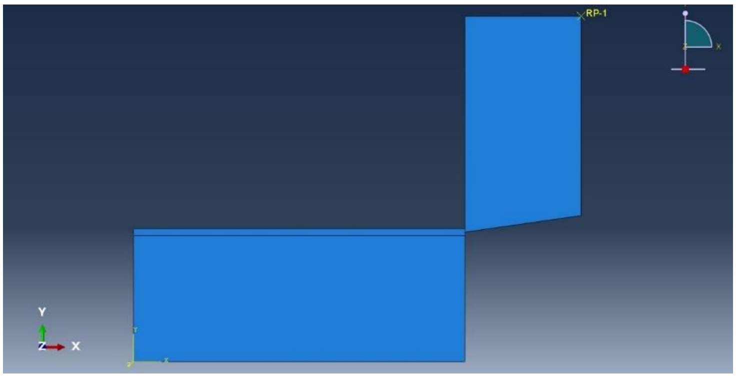

Figure 4: 2D geometrical model of orthogonal machining process in Abaqus

The tool was meshed using CPE3T element types available in the Abaqus library with the tool tip was given a radius of 0.01mm. A reference point was created on the upper right corner of the tool geometry. All nodes on the tool surface can be constrained to this reference points which enables the reference point to drive the cutting tool and act as a controlling point. ALE adaptive meshing technique was used in the upper portion of the workpiece to limit the deformation of the elements.

The tool and workpiece were assembled and a feed value of 0.05mm/rev. The interaction between tool and workpiece was defined as General Contact between the surfaces of tool and the geometrical surface of workpiece. While defining the interaction properties, the penalty contact method was defined and the co-efficient of friction of the value of 0.5 was used.

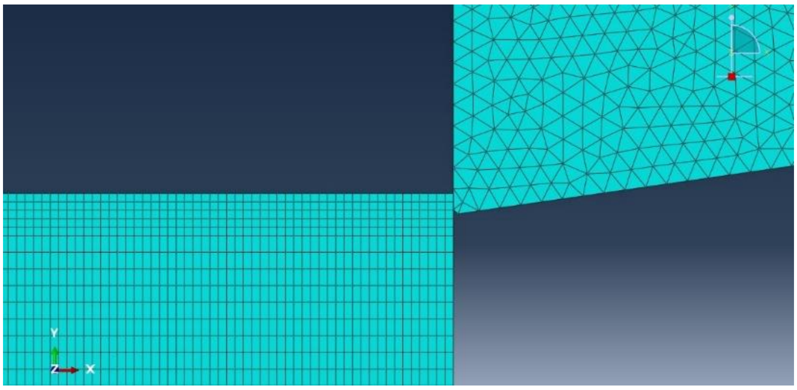

Figure 5: Interaction between tool tip and workpiece

3.2 Applying Boundary conditions

Different boundary conditions were defined to replicate the machining conditions. The workpiece was fixed, and its motion was restricted in all direction. Only the motion of tool in x-axis was allowed while its motion in Y-axis and around an axis were also restricted. The cutting speed was provided in the form of tool velocity in negative x-axis to the reference point of the tool.

Tool was modelled as a rigid body by applying constraint and the reference point was coupled to the surface of the tool geometry by applying the Kinematic coupling constraint. Thus, coupling the entire geometry of the tool (in all 3 degree of freedom) to the single reference point.

As the experiment was carried out at a temperature equivalent to room temperature. So, the predefined initial conditions of temperature of 25^{o}C were applying to both. The step time of this process was calculated using the cutting speed and depth of cut. Properties of materials for workpiece and tool were defined manually and created in the software library.

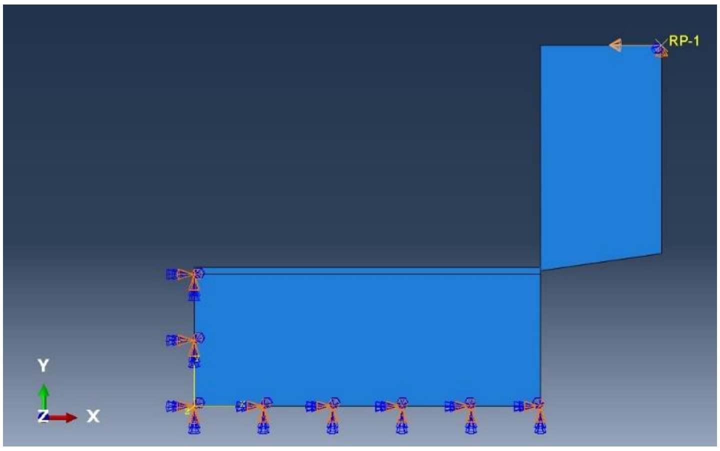

Figure 6: Applying Boundary conditions and loading conditions

The material modeling and definition will be discussed in the next portion. Once all the parameters had been defined in the software, the simulation was ready to be tested.

3.3 Material modelling

The material modelling is a fundamental step which defines the accuracy of results of simulation. Material of the cutting tool is Tungsten Carbide. Since we constrained the tool as a rigid body not going through any plastic deformation so only the elastic properties and strength of the tool was relevant for modelling.

The properties of Tungsten Carbide are defined as follows:

Table 3: Material Properties of Tungsten Carbide

Parameter	**WC**
Density	15700 (Kg / m^3)
Specific heat	178 (J/Kg/^{o}C)
Poisson Ratio	0.23
Young's Modulus	705000 (MPa)
Thermal conductivity	24 (W/m^{o}C)

The material assigned to the workpiece in this process is Inconel 718. Since the workpiece goes through elastic as well as plastic deformation and gets damaged due to the machining process so the definition of workpiece material involves more detail than the tool material.

The Young's Modulus and specific heat on Inconel 718 have a tendency to change with the rise in temperature so values on certain temperature were adopted from [11] for better accuracy of the simulation.

Table 4: Modulus of Elasticity for Inconel-718

Modulus of Elasticity	**Poisson ratio**	**Temperature**
217	0.3	20
155.9	0.3	871

The density of Inconel 718 was taken as 8220 Kg/m^3. The inelastic heat fraction was taken to be 0.9.

The plastic deformation behavior of the workpiece material was defined using the Johnson Cook plasticity model as it is most commonly used for high strain rate deformation problems. The equation for Johnson Cook model plasticity model is as follows:

$$\sigma = (A + B\varepsilon^n)(1 + C\ln\frac{\dot{\varepsilon}}{\dot{\varepsilon}})(1 - \left(\frac{T - T_{room}}{T_{melt} - T_{room}}\right)^m)$$

where A is yield strength, B is strain hardening parameter, C is strain rate constant, n is strain hardening exponent, m is the thermal softening exponent while T_{room} represents room temperature and T_{melt} represents melting temperature and T stands for current temperature.

Various values of A, B, C, n and m are available in the literature and changing them can have an effect on the output values of the simulation. For the testing of each subsequent JC model the parameters of individual model were entered in the Abaqus while keeping all the other parameters of the simulation same. Thus, to obtain a better understanding of the outputs by changing the input JC plasticity model.

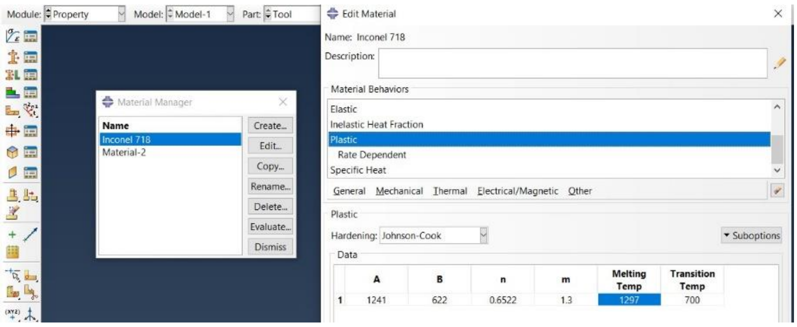

Figure 7: Defining JC parameters in Abaqus

The damage initiation and evolution in the workpiece was define by using the Johnson cook damage model, which gives the equivalent strain at failure by this equation:

$$\varepsilon_f = \left[\left(D_1 + D_2 \exp\left(D_3 \frac{P}{\sigma}\right)\left(1 + D_4 ln \frac{\varepsilon_{pl}}{\varepsilon_0}\right)\right)\right][1 + D_5(\frac{T - T_r}{T_m - T_r})]$$

Where D1 - D5 are damage which are determined at transition temperature. These values are obtained experimentally and in this simulation they have been taken from literature [22] The simulation was conducted at 3 different cutting speeds of 20, 40, 80 m/min to obtained results at different variations.

The accuracy of this FEM simulation can be confirmed by comparison of its results with experimentally obtained values. The experimental results of this machining process have been obtained from [11] in which the machining of Inconel 718 was performed under similar conditions so these experimental results can be used as a benchmark to check which JC plasticity model predicts the cutting forces closest to the experimental values.

Chapter 4: Evaluation of different Models using Abaqus

There are several values for the parameters of involved in the equation for J-C plasticity model available in the literature which can be used to define the plastic deformation and dynamic behavior of the material during machining. However, the purpose of this research is to find out which model provides us with results approximate to the experimentally derived results for cutting force and feed force obtained by the actual machining of Inconel 718.

For this purpose, following J-C model parameters values have been selected from different available published research articles for the evaluation and comparison.

Table 5: Values of parameters of JC Material Model available in literature

Model No.	**A (MPa)**	**B (MPa)**	**n**	**m**	**C**	$\dot{\varepsilon}$	**Literature reference**
1	980	1370	0.164	1.03	0.02	0.001	[7]
2	1290	895	0.526	1.55	0.016	0.03	[15]
3	1200	1284	0.54	1.2	0.006	0.001	[16]
4	1485	904	0.777	1.689	0.015	0.001	[11]
5	1562	300	0.25	1.7	0.0164	1	[15]
6	450	1700	0.65	1.3	0.017	1	[8]
7	860	1100	0.5	1.05	0.0082	0.001	[17]
8	1241	622	0.6522	1.3	0.0134	1	[18]

The rest of the inputs in the simulation were kept same for each iteration during the evaluation process. Only the JC plastic deformation parameters were changed according to the given arrangement of models so the effect of using different material models, as input, on the resultant cutting and feed forces acting on tip of the cutting tool can be observed during evaluation procedure.

For the comparison of outputs obtained from simulation, experimental results of orthogonal machining process for Inconel 718 has been referred to from [11] and it acts as a benchmark for comparison with the results of simulation. The simulation was carried out at the same cutting speeds with the same tool tip radius as selected in the experimental process for making the comparison accurate. orthogonal cutting tests were performed at the WZL at RWTH Aachen University using the machine model Forst RASX 8x2200x600M/CNC. TTo compare the results of cutting and feed forces obtained in 3D with the 2D simulation. The results were divided by the value of thickness of workpiece (3.5 mm). The experimental data for cutting forces and feed forces is as shown in the following table 6:

Table 6: Experimental results of cutting forces and feed forces with tool radius 10 µm.

Cutting Speed (m/min)	**Cutting Force (N)**	**Feed Force (N)**
20	269	235
40	234	192
80	232	181

4.1 Results and discussion

Results of cutting and feed forces from the FEA simulation model of orthogonal machining process are as following in comparison with the experimental values.

4.1.1 Cutting Force

For calculation of cutting force on the tool during the simulation, the average value of cutting force is taken from the output forces obtained over time during overall step time. The comparison of average cutting force obtained during the simulation using each set of parameters of JC model as input and the experimental values are as follows:

Table 7-a: Comparison of cutting force values using Model 1 as input

Model	**Cutting Speed (m/min)**	**Cutting Force (N) Experimental**	**Cutting Force (N) Simulation**	**Error %**
M1	20	269	279	3.72
	40	234	244	4.27
	80	232	261	12.5

Table 7-b: Comparison of cutting force values using Model 2 as input

Model	Cutting Speed (m/min)	Cutting Force (N) Experimental	Cutting Force (N) Simulation	Error %
M2	20	269	287	6.68
	40	234	264	12.8
	80	232	270	16.4

Table 7-c: Comparison of cutting force values using model 3 as input

Model	Cutting Speed (m/min)	Cutting Force (N) Experimental	Cutting Force (N) Simulation	Error %
M3	20	269	291	8.18
	40	234	270	15.4
	80	232	260	12.1

Table 7-d: Comparison of results using model 4 as input

Model	Cutting Speed (m/min)	Cutting Force (N) Experimental	Cutting Force (N) Simulation	Error %
M4	20	269	294	9.29
	40	234	246	5.13
	80	232	250	7.76

Table 7-e: Comparison of cutting force values using model 5 as input

Model	Cutting Speed (m/min)	Cutting Force (N) Experimental	Cutting Force (N) Simulation	Error %
M5	20	269	276	2.6

	40	234	255	8.97
	80	232	253	9.05

Table 7-f: Comparison of cutting force values using model 6 as input

Model	**Cutting Speed (m/min)**	**Cutting Force (N) Experimental**	**Cutting Force (N) Simulation**	**Error %**
M6	20	269	231	-14.1
	40	234	267	14.1
	80	232	254	9.48

Table 7-g: Comparison of cutting force values using model 7 as input

Model	**Cutting Speed (m/min)**	**Cutting Force (N) Experimental**	**Cutting Force (N) Simulation**	**Error %**
M7	20	269	241	-10.4
	40	234	217	-7.26
	80	232	212	-8.62

Table 7-h: Comparison of cutting force values using model 8 as input

Model	**Cutting Speed (m/min)**	**Cutting Force (N) Experimental**	**Cutting Force (N) Simulation**	**Error %**
M8	20	269	257	-4.46
	40	234	240	2.56
	80	232	237	2.16

The results obtained related to cutting force using these eight models show that using different models has a considerable impact on the output values of cutting force acting on cutting tool and this FEA simulation is able to give the results with different accuracies using these models.

Table 7-a to 7-h represent the comparison between simulated average cutting force and experimal cutting force while using different set of JC parameters as input in FEA model at different cutting speeds. Most of the input models overestimated or underestimated the

At 20 m/min:

For the speed of 20 m/min, the cutting force is overestimated using the model M1,M2,M3,M4,M5. With the highest difference being recorded at 9% using M4 as input and lowest difference at 2.6% by using M5. The other models underestimed the value with a highest difference of -14 % using M6 and lowest at -4.46% using M8.

At 40 m/min:

For the speed of 40 m/min, the cutting force is underestimated by -7% using M7 while other input models overestimeated the result with the highest value of difference at 15% using M3 and lowest difference was 2.56% using M8.

At 80 m/min

For the speed of 80 m/min, the output is underestimated by a value of -8% by M7 while all other models resulted in overestimation of the cutting force with the highest margin being 16% by M2 and lowest difference being 2.1% using M8 as an input.

By observing the results of all set of paramters and their corresponding output values it is evident that the accuracy of results obtained by using M8 as input was least affected by the changed in cutting speed, it was able to predict the cutting forces during the cutting process with lowest difference when compared with the experimental values at the given 3 settings of cutting speeds.

M1 was able to predict the results with low diffenece at low speed settings however its accuracy dropped significantly at high speed setting of 80 m/min thus it proves to be less accurate as compared to M8.The highest differences were recorded by M2 thus reducing the accuracy of the FEA model.

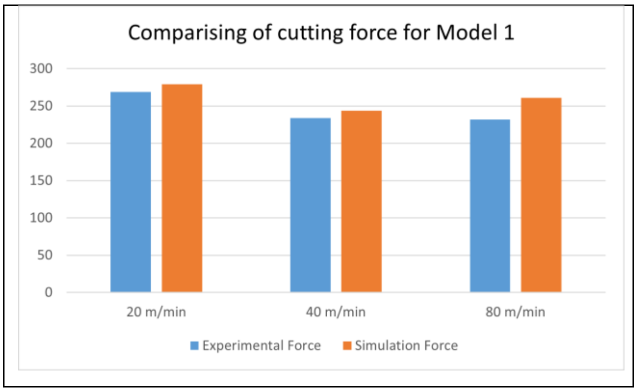

(a)

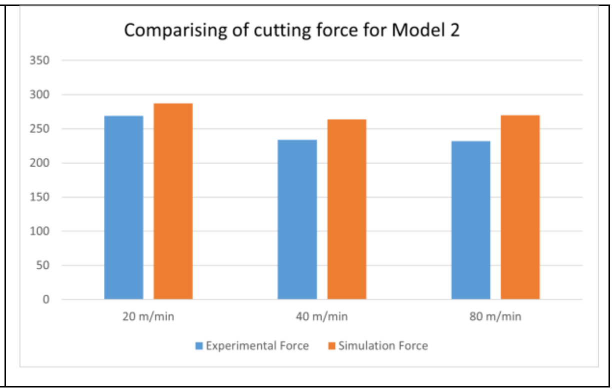

(b)

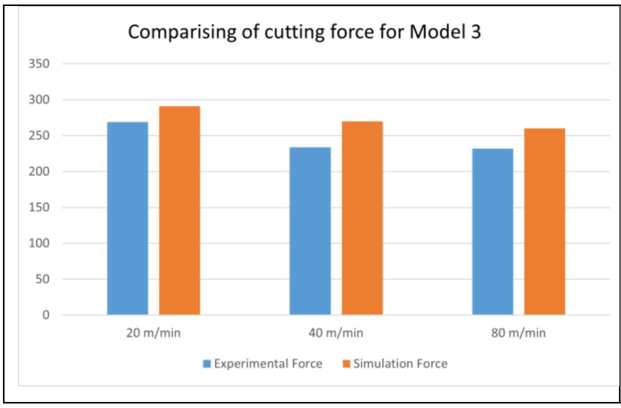

(c)

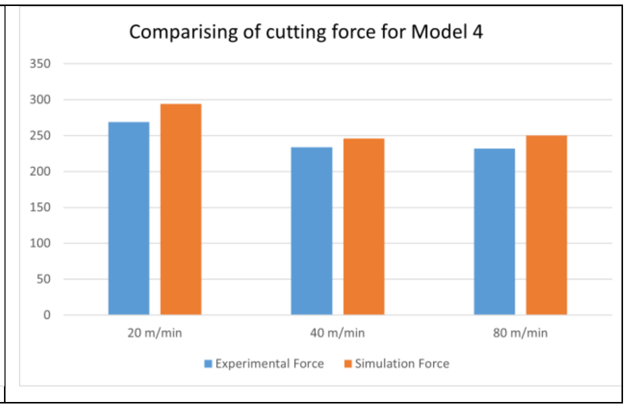

(d)

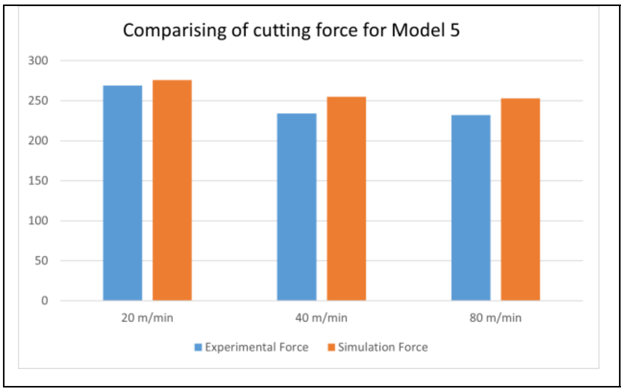

(e)

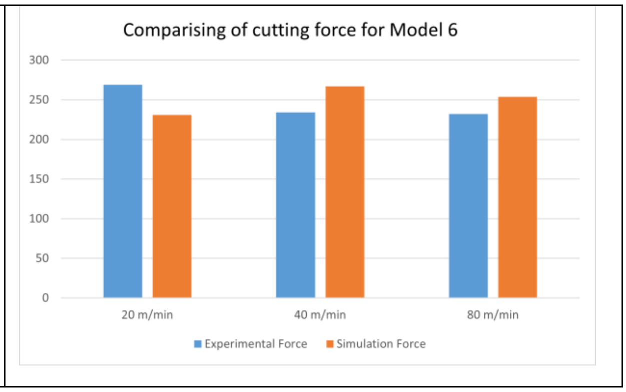

(f)

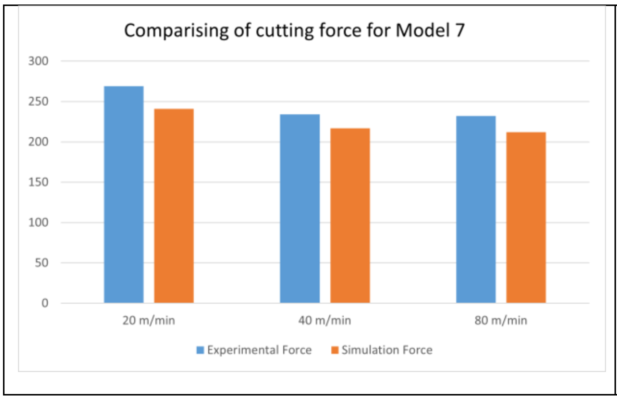

(g)

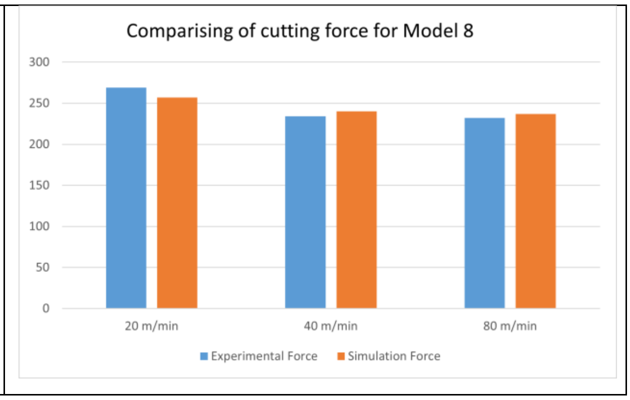

(h)

Figure 8: Graphical representation of cutting force result with Force (N) on y axis

4.1.2 Feed Force:

The average value of feed force during the complete step time was calculated for each constitutive model and the results of feed force at designated cutting speeds obtained from the FEM simulation as compared to the experimentally obtained values for all the identified JC models is as follows:

Table 8-a: Comparison of feed force values using model 1 as input

Model	**Cutting Speed (m/min)**	**Feed Force (N) Experimental**	**Feed Force (N) Simulation**
M1	20	235	153
	40	192	136
	80	181	125

Table 8-b: Comparison of feed force values using model 2 as input

Model	**Cutting Speed (m/min)**	**Feed Force (N) Experimental**	**Feed Force (N) Simulation**
M2	20	235	161
	40	192	132
	80	181	125

Table 8-c: Comparison of feed force values using model 3 as input

Model	**Cutting Speed (m/min)**	**Feed Force (N) Experimental**	**Feed Force (N) Simulation**
M3	20	235	192
	40	192	163
	80	181	156

Table 8-d: Comparison of feed force values using model 4 as input

Model	Cutting Speed (m/min)	Feed Force (N) Experimental	Feed Force (N) Simulation
M4	20	235	190
	40	192	148
	80	181	145

Table 8-e: Comparison of feed force values using model 5 as input

Model	Cutting Speed (m/min)	Feed Force (N) Experimental	Feed Force (N) Simulation
M5	20	235	149
	40	192	134
	80	181	125

Table 8-f: Comparison of feed force values using model 6 as input

Model	Cutting Speed (m/min)	Feed Force (N) Experimental	Feed Force (N) Simulation
M6	20	235	179
	40	192	164
	80	181	157

Table 8-g: Comparison of feed force values using model 7 as input

Model	Cutting Speed (m/min)	Feed Force (N) Experimental	Feed Force (N) Simulation
M7	20	235	148
	40	192	112
	80	181	114

Table 8-h: Comparison of feed force values using model 8 as input

Model	Cutting Speed (m/min)	Feed Force (N) Experimental	Feed Force (N) Simulation
M8	20	235	152
	40	192	139
	80	181	134

The results obtained through this method show that different models were able to predict the feed force with different accuracies.

Feed Forces have been underestimated as compared to the experimental results. This issue has been faced by other researchers as well. The most likely reason can be that the tool wear is not accounted for in the simulation process. Among these models, M3 was able to predict the feed forces with the lowest difference while M5 gave the highest error percentage. The remaining models underestimated the values with almost similar margin of error. [19] also discussed the underestimation of feed forces during simulation machining process and suggested another possible reason for this underestimation that this effect could be due to the defining the interaction between the tool and chip using simple Coulomb friction model. The focus of this research work was to evaluate the models on the basis of cutting force results thus the selection of model will be carried out on the model with showing comparatively more accuracy in the cutting force results.

The graphical representation of feed forces results in comparison to the experimentally obtained values is shown in the figures 9 (a-h).

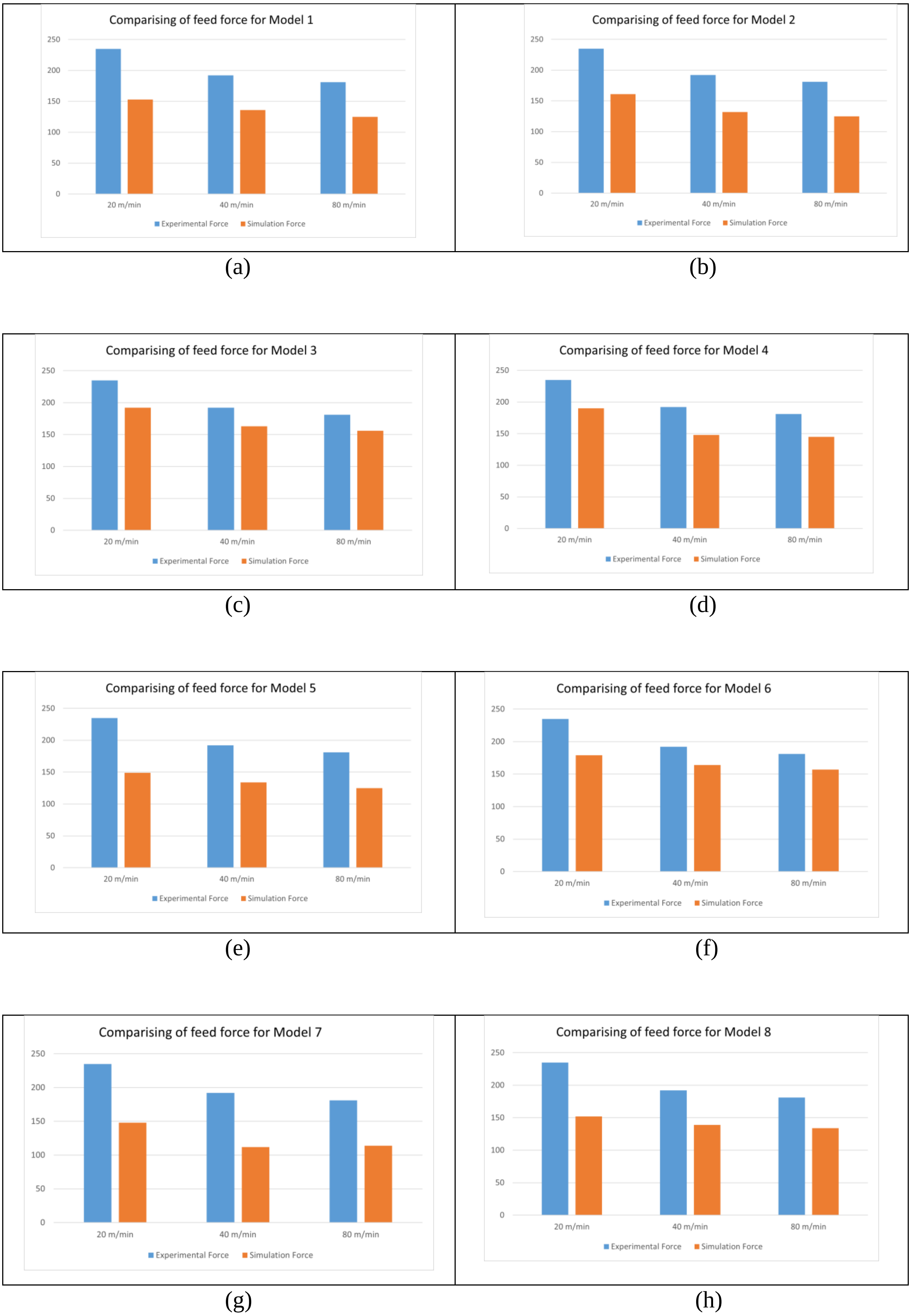

Figure 9: Graphical representation of feed force results with Force (N) on Y axis

Chapter 5: Conclusion

In the current research, a finite element 2-dimensional simulation model for orthogonal machining of Inconel 718 was developed using Abaqus. The cutting forces and feed forces were calculated using the different sets of parameters of JC material model available in the literature to determine which one of them can predict the forces with more accuracy. The simulation was carried out at 3 different settings of cutting speeds of 20 m/min, 40 m/min, 80 m/min with a feed value of 0.05 mm. The results of simulation were validated by corresponding experimental values.

For the given set of parameters of JC material model, it was found that M8 was able to predict the results with more accuracy as compared to other models and these values of JC parameters can be used while simulating and studying the machining process of Inconel-718 with greater accuracy.

This model can also be used as an alternate for experimental machining process to save cost and study the phenomena further to optimize the process. This simulation was able to calculate the cutting forces, which are the largest component of force acting on the tool in terms of magnitude, with a very small difference with experimental results acting as a benchmark. However, the underestimation of feed forces is an issue which should be studied further.

References

[1] J. I. Hughes, A. R. C. Sharman, and K. Ridgway, “The effect of cutting tool material and edge geometry on tool life and workpiece surface integrity,” *Proc. Inst. Mech. Eng. Part B J. Eng. Manuf.*, vol. 220, no. 2, pp. 93–107, 2006, doi: 10.1243/095440506X78192.

[2] R. Asmatulu, “Nanocoatings for corrosion protection of aerospace alloys,” *Corros. Prot. Control Using Nanomater.*, pp. 357–374, 2012, doi: 10.1016/B978-1-84569-949-9.50014-9.

[3] “Introduction to aerospace materials,” *Introd. to Aerosp. Mater.*, pp. 1–14, 2012, doi: 10.1533/9780857095152.1.

[4] S. H. I. Jaffery and P. T. Mativenga, “Wear mechanisms analysis for turning Ti-6Al-4V-towards the development of suitable tool coatings,” *Int. J. Adv. Manuf. Technol.*, vol. 58, no. 5–8, pp. 479–493, 2012, doi: 10.1007/s00170-011-3427-y.

[5] J. Scully, “Elsevier materials selector,” *Corros. Sci.*, vol. 33, no. 6, pp. 1001–1005, 1992, doi: 10.1016/0010-938x(92)90062-8.

[6] M. Range and C. Temperature, “Special Metals Inconel G-3,” *Alloy Dig.*, vol. 70, no. 8, 2021, doi: 10.31399/asm.ad.ni0774.

[7] G. Chandra Mouli, K. Prakash Marimuthu, and T. Jagadeesha, “2D Finite Element Analysis of Inconel 718 Under Turning Processes,” *IOP Conf. Ser. Mater. Sci. Eng.*, vol. 912, no. 3, 2020, doi: 10.1088/1757-899X/912/3/032021.

[8] P. Niesłony, W. Grzesik, and K. Zak, “Numerical simulation and experimental verification of friction in turning inconel 718 alloy,” *Proc. 8th Int. Conf. Lead. Edge Manuf. 21st Century, LEM 2015*, no. March, 2015, doi: 10.1299/jsmelem.2015.8._2301-1_.

[9] “About ALE adaptive meshing.” https://abaqus-docs.mit.edu/2017/English/SIMACAEANLRefMap/simaanl-c-aleover.htm

[10] G. R. Johnson and W. H. Cook, “Fracture characteristics of three metals subjected to various strains, strain rates, temperatures and pressures,” *Eng. Fract. Mech.*, vol. 21, no. 1, pp. 31–48, 1985, doi: 10.1016/0013-7944(85)90052-9.

[11] R. Bedzra, “Finite element simulation of two dimensional orthogonal cutting process

and comparison with experiments," no. August, 2013.

[12] C. Kilicaslan, "Modelling and Simulation of Metal Cutting By Finite Element Method," *Strain*, no. December, p. 86, 2009.

[13] A. Ali, B. El Hossainy, and C. Abd-Rabou, "Finite Element Method Based Modeling for Tool Wear Prediction in Orthogonal Cutting Process," *J. Eng. Sci. Mil. Technol.*, vol. 17, no. 17th International Conference, pp. 1–14, 2017, doi: 10.21608/ejmtc.2017.21079.

[14] R. S. Pawade, S. S. Joshi, P. K. Brahmankar, and M. Rahman, "An investigation of cutting forces and surface damage in high-speed turning of Inconel 718," *J. Mater. Process. Technol.*, vol. 192–193, pp. 139–146, 2007, doi: 10.1016/j.jmatprotec.2007.04.049.

[15] F. Jafarian, M. Imaz Ciaran, D. Umbrello, P. J. Arrazola, L. Filice, and H. Amirabadi, "Finite element simulation of machining Inconel 718 alloy including microstructure changes," *Int. J. Mech. Sci.*, vol. 88, pp. 110–121, 2014, doi: 10.1016/j.ijmecsci.2014.08.007.

[16] B. Erice Echávarri, "Flow and Fracture Behaviour of High Performance Alloys," p. 242, 2012.

[17] I. U. Haq, G. Weiguo, M. Arif, and M. Z. Sheikh, "Study of Various Conical Projectiles Penetration into Inconel-718 Target," *Procedia Struct. Integr.*, vol. 13, pp. 1955–1960, 2018, doi: 10.1016/j.prostr.2018.12.265.

[18] T. Ozel, I. Llanos, J. Soriano, and P. J. Arrazola, "3d finite element modelling of chip formation process for machining inconel 718: Comparison of FE software predictions," *Mach. Sci. Technol.*, vol. 15, no. 1, pp. 21–46, 2011, doi: 10.1080/10910344.2011.557950.

[19] S. L. Soo, D. K. Aspinwall, and R. C. Dewes, "3D FE modelling of the cutting of Inconel 718," *J. Mater. Process. Technol.*, vol. 150, no. 1–2, pp. 116–123, 2004, doi: 10.1016/j.jmatprotec.2004.01.046.

[20] H. A. Soliman, A. Y. Shash, T. M. El-Hossainy, and M. Abd-Rabou, "Cutting forces and crater wear prediction in orthogonal cutting using two approaches of finite element modeling," *Eng. Reports*, vol. 2, no. 10, pp. 1–18, 2020, doi: 10.1002/eng2.12240.

[21] H. A. Soliman, A. Y. Shash, T. M. El Hossainy, and M. Abd-Rabou, "Investigation of

process parameters in orthogonal cutting using finite element approaches," *Heliyon*, vol. 6, no. 11, p. e05498, 2020, doi: 10.1016/j.heliyon.2020.e05498.

[22] X. Wang, C. Huang, B. Zou, H. Liu, H. Zhu, and J. Wang, "Dynamic behavior and a modified Johnson-Cook constitutive model of Inconel 718 at high strain rate and elevated temperature," *Mater. Sci. Eng. A*, vol. 580, pp. 385–390, 2013, doi: 10.1016/j.msea.2013.05.062.